Spinodal Clustering in Thin Films of Nanoparticle-Polymer Mixtures

Him Cheng Wong and João T. Cabral*

Department of Chemical Engineering, Imperial College London, London SW7 2AZ, United Kingdom
(Received 23 October 2009; revised manuscript received 18 May 2010; published 12 July 2010)

Thin supported polystyrene-C_{60} fullerene mixtures annealed above their glass transition temperature develop spinodal surface undulations which depend on film thickness h(20–500 nm), polymer molecular mass M_w, temperature, and time t. The dominant wavelength $\lambda \sim 1$–10 μm scales linearly with h and coarsening kinetics follow $\lambda \sim t^{\alpha}$, with $0 < \alpha(h) < 1/3$; the morphology eventually pins at long times. This spinodal surface excitation contrasts with dewetting suppression and film stability observed in low-M_w polymers and results from the interplay of binary miscibility and fullerene substrate attraction.

Understanding the stability of polymer nanocomposite thin films is both scientifically and technologically important due to their ubiquitous applications in organic electronics and photovoltaics, coatings, and adhesives [1].

The discovery that C_{60} fullerenes could suppress the dewetting of thin polystyrene (PS) films [2] first demonstrated that the addition of trace amounts of nanoparticles (NPs) could provide a route to uniform, stable polymer films and has therefore attracted great interest in recent years. Numerous studies of thin supported films with additives such as C_{60} [2,3], dendrimers [4], and cross-linked polymeric NPs [3,5] have established that the surface attraction of NPs to the substrate interface can yield a diffuse interfacial layer that shields polymer-interface interactions, pins the contact lines of growing holes, and thus inhibits dewetting of ultrathin films. This entropically driven NP segregation mechanism [6] is analogous to the "depletion attraction" [7] responsible for NP migration to cracks and crazes [1,8].

In this Letter, we report a spinodal surface excitation that emerges in high-molecular mass M_w PS-C_{60} nanocomposite thin films, annealed above their glass transition temperature T_g, shown in Fig. 1(f). The characteristic wavelength of the dominant mode λ^* and the time evolution of the surface morphology have been examined as a function of film thickness h, annealing temperature T, and polymer molecular mass M_w. This "spinodal clustering" process is investigated in terms of fluid phase separation and nanoparticle surface attraction.

Uniform nanocomposite polystyrene-C_{60} films were prepared from dilute solution and spun-cast onto silicon wafers. PS and C_{60} Fullerene NPs (MER 99 + %) were separately dissolved in toluene (99.8 + %), sonicated for 30 min, and mixed to obtain a 5% mass fraction of C_{60}. PS of M_w 2.75, 10, 80, and 270 kg/mol ($M_w/M_n = 1.1$, 1.05, 1.05, and 2.4) was obtained from Polymer Source, Polymer Labs, and BP Chemicals; their radii of gyration (R_g) are, respectively, 1.4, 2.7, 7.6, and 14 nm and the diameter of C_{60} is ≈ 0.7 nm. Solutions were further sonicated for 30 min and filtered (0.45 μm) before spin-casting onto

[100] silicon wafers with a native (≈ 2 nm) oxide layer, as probed by x-ray reflectometry (PANAlytical X'Pert PRO). Control experiments were carried out on piranha-cleaned wafers [2,3] that result in stable (neat) PS thin films [9]. Film thickness h, measured by uv-visible interferometry (Filmetrics, F20-UV), ranged from 20 to 500 nm. Films were dried at room temperature for 24 h and then isothermally annealed *in situ* (up to 72 h) on a hot stage mounted on a reflection optical microscope (Olympus BX41M). Prior to annealing, all films are flat and uniform. The surface topography was further charac-
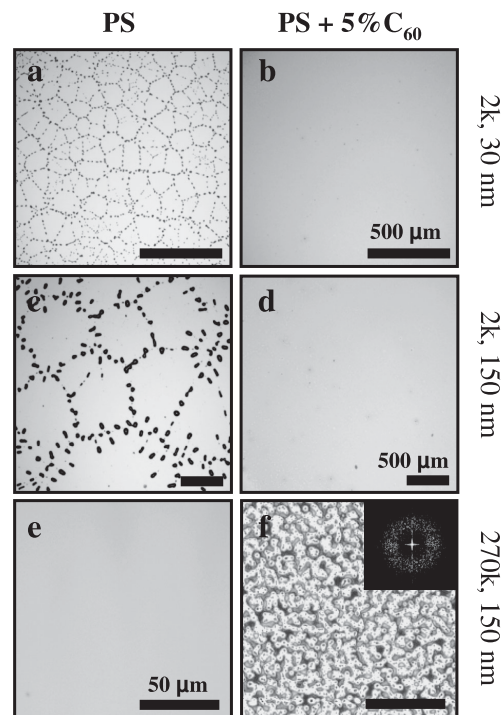
PS **PS + 5% C_{60}**

FIG. 1. Optical micrographs of neat PS and PS − 5%C_{60} nanocomposite thin films upon annealing for 30 min at 140 °C (a),(b) and 180 °C (c)–(f). Film thickness: (a),(b) 30 nm; (c)–(f) 150 nm. Inset (f) shows FFT of spinodal clustering morphology [scale bars: (a)–(d) 500 μm, (e),(f) 50 μm].

terized by tapping-mode atomic force microscopy (AFM) (Innova, Veeco, TESP-SS probes). Structure factors $S(q)$ were obtained by thresholding, fast-Fourier-transform (FFT), and radially averaging the optical micrographs, while cluster area fraction, size, and number distribution was carried by image analysis (National Instruments). The characteristic wavelength of the surface morphology is obtained by $\lambda^* = 2\pi/q^*$, where q^* is the wave number corresponding to the maximum intensity of $S(q)$. The growth kinetics of the in-plane structure $\lambda^*(t)$ were investigated as a function of annealing time (t), film thickness h, and mass M_w (above and below entanglement $M_e \sim$ 10 kg/mol). For comparison, neat PS films were investigated in the same experimental conditions.

For consistency, we first reproduce the observations of Barnes *et al.* [2] and confirm the suppression of dewetting in low-M_w PS films upon addition of C_{60}. Figure 1(a) depicts the usual Voronoi dewetting pattern [10], observed for a PS(2k), $h = 30$ nm film, annealed at 140 °C for 30 min. Dewetting is suppressed in its C_{60}-filled counterpart, shown in Fig. 1(b). This effect holds when increasing h and T to 150 nm and 180 °C, respectively, apart for the expected scaling of dewetting polygons in neat films with h [Fig. 1(c)] and emergence of isolated NP "clusters" in composite films [Fig. 1(d)]. By contrast, high-M_w nanocomposite films of PS(270k) in the same conditions exhibit a spinodal-like morphology with characteristic wavelength of $\lambda \approx 6.3$ μm, shown in Fig. 1(f). The process occurs independently of piranha-etched (PS-wetting) and native wafer (metastable) substrates. The neat PS(270k) film, on the other hand, does not dewet within this time scale and remains uniform [Fig. 1(e)] for $t \gtrsim 10$ h.

In order to elucidate the nature of this spinodal clustering process, we examine the dependence of this morphology with film thickness in Fig. 2 for PS(270k) − 5%C_{60}. The structure is discussed in terms of dominant length scale λ^* and size and number of individual clusters. The FFT are depicted in the insets in Fig. 2(a)–2(g) and show a spinodal ring that shrinks with increasing h. Figure 2(h)

compiles the structure factors as a function of thickness demonstrating a reduction in peak position q^* with increasing h, at constant t of 30 min. The individual clusters, on the other hand, increase in size (ranging from radius of approximately 200 to 1000 nm) but decrease in number with film h. The surface area fraction occupied by the clusters in the 170 nm nanocomposite film $\sim 5.3 \pm 0.5\%$ is in agreement with the overall C_{60} mass fraction.

The 3D topography revealed by AFM [Fig. 2(i)] confirms that the nanocomposite films do not dewet the substrate within the time scales investigated. Instead, undulating surface patterns of large amplitude develop with time, reaching in excess of 300 nm at late stages (for $h \sim 150$ nm). FFT of AFM topography scans and binary optical micrographs yields identical dominant λ, indicating that optical thresholding does not induce artifacts in determining the periodicity λ. The time evolution of the surface morphology as a function of film thickness at $T = 180$ °C is summarized in Fig. 3. The structure factor of a representative 135 nm film, shown in Fig. 3(a) at selected time intervals, characterizes the coarsening kinetics of spinodal clustering.

The bicontinuous morphology suggests phase separation via spinodal decomposition. While spinodal dewetting occurs in ultrathin polymer films, including polystyrene of $h \sim 5$ nm [11,12], the present observations hold for both piranha-etched (which result in stable PS films [9]) and native wafers. Furthermore, the film thicknesses (20–500 nm) are comparatively large and AFM confirms that films do not actually dewet the substrate within experimental time scales (of 1–10 h). In contrast, the spinodal morphology develops within 2–3 min. The initial wavelength λ_0 of the structure (computed at $t_0 = 3$ min) is plotted as a function of film thickness h in Fig. 3(b) and follows $\lambda_0 \sim h^1$ in the accessible h range.

Fluid-fluid phase separation is expected in asymmetric polymer-particle mixtures [13] for large particle-to-monomer size ratios (in excess of ~ 5). As in polymer mixtures, increasing the molecular mass should increase
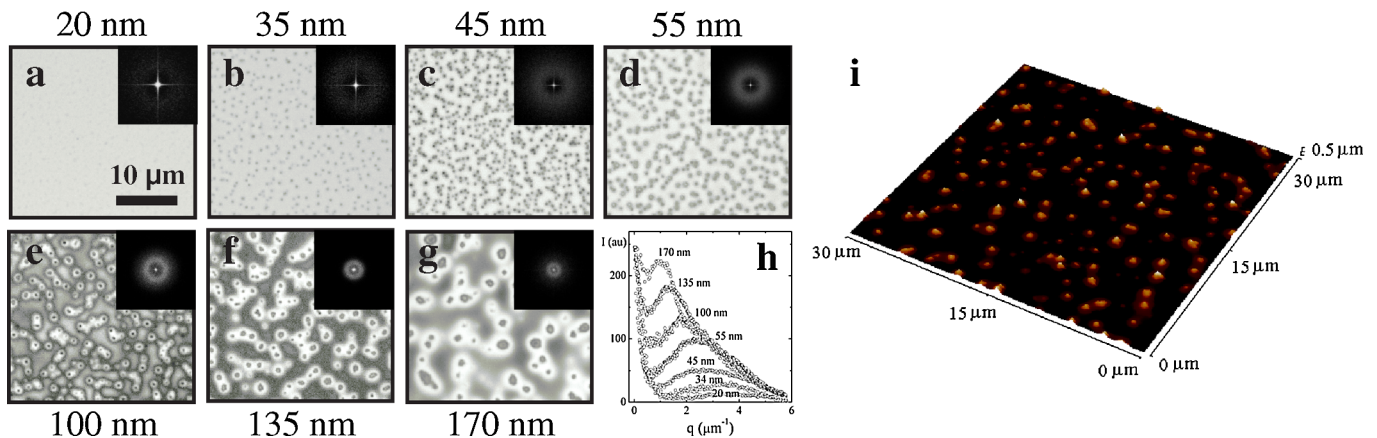

FIG. 2 (color online).   Optical micrographs of PS(270k) − 5%C_{60} mixtures of various film thicknesses (a)–(g) annealed for 30 min at 180 °C. (h) Structure factors obtained from radial average of FFT insets. (i) AFM topography scan for $h = 135$ nm (2f).
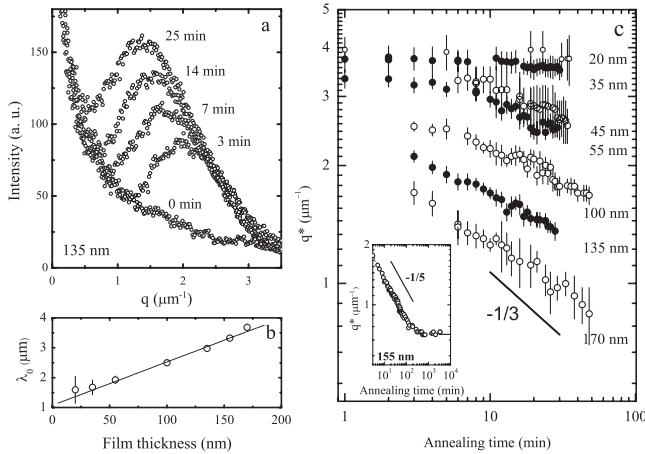
FIG. 3. (a) Time dependence of the structure factor of PS(270k) $- 5\%C_{60}$ film of $h = 135$ nm, annealed at $180\,°C$. (b) Film thickness dependence of the initial dominant wavelength $\lambda_0 \equiv 2\pi/q(t \rightarrow 0)$; line is a linear fit to h^1. (c) Coarsening kinetics of dominant wave number q^* as a function of h. The inset depicts pinning of morphology after long annealing times for selected $h = 155$ nm, yielding $\lambda_\infty = 8.7$ μm.

the critical point [14] and result in phase separation. Further, an entropically driven surface phase transition has been observed [2–4] and predicted [6] for low-M_w polymer-particle thin films, resulting in the expulsion and layering of NPs along the solid substrate. Early stages of spinodal decomposition are generally described by Cahn-Hilliard theory [15], yielding a dominant wavelength, which then grows via a number of coarsening mechanisms [16]. Thin film confinement results in 2D effects that generally reduce the coarsening power laws $\lambda \sim t^\alpha$, where exponent α is thickness-dependent, and eventually pinning of the structure at long times [17]. The initial λ_0 scales with $\sim h^1$ in phase separating thin films, compatible with present observations [Fig. 3(b)].

The time dependence of the dominant wave number q^* is shown in Fig. 3(c). As expected, thinner films generally yield smaller λ^* and coarsen comparatively slower. The thicker films (~170 nm) exhibit a $q^* \sim t^{-1/3}$ as expected for evaporation or condensation and Brownian coalescence mechanism in phase-separating fluid mixtures. The center of mass of the clusters does not move with time, while the cluster size grows, indicating that either mechanism would involve motion of submicrometer particles. This exponent decreases with decreasing h and seemingly vanishes for $h \rightarrow 20$ nm. At the initial stages, q^* appears to be time-*independent* as expected in the early stages of phase separation. At very long times, shown in the inset in Fig. 3(c), the in-plane structure eventually pins, reaching $\lambda_\infty = 8.7$ μm for the $h = 155$ nm film shown here. Further increasing h results in a qualitative morphological change characterized by polydisperse clusters and loss of spinodal character.

We rationalize these observations in terms of the entropic-driven phase separation of PS-fullerene mixtures, followed by C_{60} association, observed in the bulk above a threshold temperature [18], into a C_{60}-rich dispersed phase, enveloped by a PS-rich phase, much like in thin film polymer mixtures with asymmetric surface attraction [17].

In order to reconcile the previous reports of suppression of dewetting upon addition of nanoparticles [2,3] and the current spinodal clustering observations, we investigate the effect of M_w in Fig. 4. Neat PS films of $h \sim 135$ of all M_w studied, annealed above T_g, are metastable on native silicon oxide substrates [12]: PS(2k) and PS(10k) films rupture readily (<1 min) at $180\,°C$, while PS(80k) and PS (270k) remain largely uniform until much longer times (up
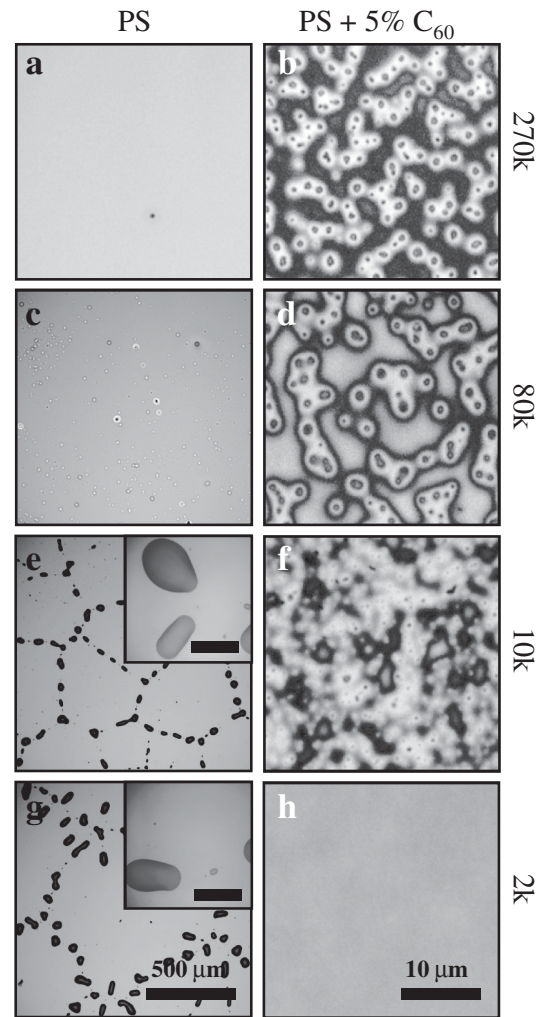

FIG. 4. Molecular mass dependence of morphology of neat and PS-C_{60} films of $h \sim 135$ nm annealed at $180\,°C$ for 30 min. Low-M_w neat PS films (e),(g) readily dewet silicon substrates, while dewetting is effectively suppressed for PS(2k) $- 5\%C_{60}$ (h) as reported previously [2,3]. Neat PS(80k) and PS(270k) (a), (c) do not dewet significantly in this time scale. Spinodal clustering occurs within 2–3 min for PS-C_{60} of higher M_w (b), (d) while intermediate M_w (10k) films (f) show a transitional morphology between stability and spinodal clustering.

to 6 and 10 h). As indicated in Fig. 1, dewetting in low-M_w PS is suppressed by addition of C_{60}. With increasing M_w, the film uniformity is gradually replaced by a bicontinuous spinodal structure. At "intermediate" molecular masses [$\sim$ entanglement mass of PS(10k)], a transition morphology is observed within ~ 1 min, resulting in nonuniform films lacking a well-defined in-plane periodicity λ.

We interpret this behavior as an interplay between polymer-particle miscibility and particle-surface attraction (or "entropic push"), which is mediated by a polymer matrix of given M_w (thus viscosity η) and film thickness. Low-M_w thin ($h \leq 30$ nm) composite films have been shown to form a diffuse C_{60} layer at the substrate interface during spin coating [2] that cannot be redispersed by solvent or thermal annealing [3]. Further, the particle entropic push depends on both particle-monomer size mismatch and configurational chain entropy, and a second surface-induced nucleation process has been predicted [6].

Neutron reflection and selective dissolution AFM studies [19] indicate that, during annealing, the integrity of the C_{60}-rich layer is maintained in low-M_w films while large clusters, anchored to the solid substrate, form in high-M_w matrices. The formation of micron-sized irregular NP clusters at the substrate interface, instead of a uniform surface monolayer, has also been recently reported on relatively thick ($h = 120$ nm) spun-cast films of PS(600k) $- 5\%C_{60}$ [20]. Nanoparticle diffusion in thin films is strongly anisotropic (considerably faster in the plane of the film direction) and the viscosity of high-M_w composite films ($\eta \sim M_w^{3.4}$ for entangled melts) correspondingly higher, tuning the interplay between surface attraction and phase separation. Fullerene clustering, in turn, leads to the undulation of surface topography, which is enriched by the PS top layer. NP surface attraction and hence the resulting surface morphology are thus highly dependent on simultaneously h and M_w. Bulk measurements corroborate the miscibility threshold of C_{60} (1%–2%) and stability temperature [18].

In summary, we report the spinodal clustering of polymer-nanoparticle thin film mixtures, resulting from the interplay of M_w-dependent binary phase separation and surface attraction. Scaling of dominant wavelength λ^* with film thickness h agrees well with linearized spinodal theories, and coarsening laws are obtained as a function of h and t. The stability boundaries depend on M_w, NP loading, thickness, temperature, and surface energy, as well as on the film depth profile structure. Cluster growth is observed at lower C_{60} concentration (1%–2%), eventually merging into a spinodal morphology after approximately 48 h at 180 °C at 2% C_{60}, albeit in smaller numbers. The generality of this process is confirmed by analogous association phenomena in other acrylate and styrenic polymer matrices [21]. Understanding this self-assembly process is essential to growing technological applications of polymer-NP coatings and thin films.

*j.cabral@imperial.ac.uk

[1] A. C. Balazs, T. Emrick, and T. P. Russell, Science **314**, 1107 (2006); R. A. Vaia and E. P. Giannelis, MRS Bull. **26**, 394 (2001); T. C. Merkel et al., Science **296**, 519 (2002); M. E. Mackay et al., Nature Mater. **2**, 762 (2003); Science **311**, 1740 (2006).

[2] K. A. Barnes, A. Karim, J. F. Douglas, A. I. Nakatani, H. Gruell, and E. J. Amis, Macromolecules **33**, 4177 (2000).

[3] M. A. Holmes, M. E. Mackay, and R. K. Giunta, J. Nanopart. Res. **9**, 753 (2007); M. A. Yaklin, P. M. Duxbury, and M. E. Mackay, Soft Matter **4**, 2441 (2008).

[4] M. E. Mackay et al., Langmuir **18**, 1877 (2002).

[5] R. S. Krishnan et al., J. Phys. Condens. Matter **19**, 356003 (2007).

[6] E. S. McGarrity et al., Phys. Rev. Lett. **99**, 238302 (2007); E. S. McGarrity, A. L. Frischknecht, and M. E. Mackay, J. Chem. Phys. **128**, 154904 (2008).

[7] J. Y. Lee, G. A. Buxton, and A. C. Balazs, J. Chem. Phys. **121**, 5531 (2004).

[8] S. Gupta, Q. Zhang, T. Emrick, A. C. Balazs, and T. P. Russell, Nature Mater. **5**, 229 (2006); J. Y. Lee, Q. Zhang, T. Emrick, and A. J. Crosby, Macromolecules **39**, 7392 (2006).

[9] P. Muller-Buschbaum, Eur. Phys. J. E **12**, 443 (2003).

[10] G. Reiter, Phys. Rev. Lett. **68**, 75 (1992); Langmuir **15**, 2551 (1999)

[11] R. Xie, A. Karim, J. F. Douglas, C. C. Han, and R. A. Weiss, Phys. Rev. Lett. **81**, 1251 (1998).

[12] R. Seemann, S. Herminghaus, and K. Jacobs, Phys. Rev. Lett. **86**, 5534 (2001).

[13] P. Paricaud, S. Varga, and G. Jackson, J. Chem. Phys. **118**, 8525 (2003); G. J. Fleer and R. Tuinier, Adv. Colloid Interface Sci. **143**, 1 (2008); J. B. Hooper, K. S. Schweizer, T. G. Desai, R. Koshy, and P. Keblinski, J. Chem. Phys. **121**, 6986 (2004).

[14] J. Dudowicz, J. F. Douglas, and K. F. Freed, J. Phys. Chem. B **113**, 3920 (2009).

[15] J. W. Cahn and J. E. Hilliard, J. Chem. Phys. **31**, 688 (1959).

[16] J. D. Gunton, M. San-Miguel, and P. S. Sahni, in *Phase Transitions and Critical Phenomena*, edited by C. Domb and J. L. Lebowitz (Academic, New York, 1983), Vol. 8, pp. 267.A. J. Bray, Adv. Phys. **43**, 357 (1994).

[17] L. Sung, A. Karim, J. F. Douglas, and C. C. Han, Phys. Rev. Lett. **76**, 4368 (1996); B. D. Ermi, A. Karim, and J. F. Douglas, J. Polym. Sci. B **36**, 191 (1998).

[18] H. C. Wong, A. Sanz, J. F. Douglas, and J. T. Cabral, J. Mol. Liq. **153**, 79 (2010).

[19] Selective dissolution of PS by tetrahydrofuran reveals that, upon annealing in high-M_w matrices, large clusters are anchored on the substrate and retain the overall spinodal morphology.

[20] J. T. Han, G.-W. Lee, S. Kim, H.-J. Lee, J. F. Douglas, and A. Karim, Nanotechnology **20**, 105705 (2009).

[21] H. C. Wong and J. T. Cabral (to be published).